Revista Mexicana de Astronomía y Astrofísica, **33**, 97–105 (1997)

MODELS FOR THE EXCRETION DISKS OF B[e] SUPERGIANTS

A. R. R. de Carvalho[1] and F. X. de Araújo

CNPq-Observatório Nacional, DAGE, Rio de Janeiro, Brazil

Received 1997 January 22; accepted 1997 June 9

RESUMEN

Estudiamos modelos de vientos radiativos con distorsión rotacional impulsados por líneas ópticamente delgadas. Presentamos las ecuaciones básicas y algunos casos particulares se aplican a discos ecuatoriales de estrellas supergigantes B[e]. Los modelos toman en cuenta el parámetro de viscosidad que simula efectos viscosos en la ley de rotación y se consideran algunos perfiles ad-hoc de temperatura. Las velocidades de expansión observadas ($V_{exp} \approx 100$ km s^{-1}) pueden ser reproducidas si: (i) el número de líneas de impulsión es cercano al máximo que se admite a partir de consideraciones de orden físico o si (ii) existe un incremento de temperatura en toda la envolvente. Las conclusiones sugieren que las fuerzas radiativas de líneas delgadas pueden ejercer un papel significativo en la dinámica de los discos de excreción en las supergigantes B[e].

ABSTRACT

Rotationally-distorted radiative wind models driven by optically thin lines are examined. The basic equations are presented and some particular cases are applied to B[e] supergiant equatorial disks. We have taken into account a viscosity parameter, which simulates viscous effects in the rotational law, and we considered some ad-hoc temperature profiles. Observational expansion velocities ($V_{exp} \approx 100$ km s^{-1}) may be reproduced if: (i) the number of driving lines is near the maximum admitted from physical considerations, or, (ii) there is a temperature increase throughout the envelope. These situations are discussed. We suggest that thin line radiative forces may play a significant role in the dynamics of B[e] excretion disks.

Key words: **STARS – MASS-LOSS — STARS – SUPERGIANTS**

1. INTRODUCTION

B[e] supergiants are massive and luminous stars. Their optical spectra are dominated by Balmer emission lines which often display a P-Cygni type profile. Narrow emission lines —permitted and forbidden— of low excitation species (mainly Fe II) are also usually seen. These lines indicate low-velocity ($v_{exp} \approx 100$ km s^{-1}) and rather cool winds. On the other hand, broad absorption lines ($v_{exp} \approx 1000$–1500 km s^{-1}) of highly ionized elements are present in the UV. In addition, they have a strong IR excess, which requires the existence of an outer dust envelope. Comprehensive reviews of their characteristics have been given by Zickgraf (1989;1993). More recently, it was shown that the B[e] phenomenon may extend to lower luminosity objects (Gummersbach, Zickgraf, & Wolf 1995).

In order to understand this hybrid spectrum, a two-component wind model was proposed by Zickgraf et al. (1986). Their empirical scenario consists of a rotating central star surrounded by a non-spherical circumstellar envelope. Roughly speaking, the envelope would be symmetric with respect to the rotation axis. According to this picture a high velocity/low density wind, typical of OB stars, is present in the polar region —where the UV lines would be mostly formed. Near the equatorial plane there would exist a much more dense and slow expansion, but with an important rotational velocity. The emission lines would be produced in this last region, sometimes referred to as the "excretion disk".

[1] Present address: Universidade Federal do Rio de Janeiro, Instituto de Física, Caixa Postal 68528, 21945-970 Rio de Janeiro, Brazil.

Such a scenario resembles qualitatively that accepted nowadays for classical Be stars (e.g., Waters & Marlborough 1994) but formation of dust must occur in the outskirts of B[e] disks.

The fast polar wind described above can be explained quite satisfactorily by "CAK-type" radiative models (Castor, Abbott, & Klein 1975; Friend & Abbott 1986; Pauldrach, Puls, & Kudritzki 1986). The radiative force in such models is essentially due to strong (optically thick) lines. Not only do they produce a high terminal velocity but also there is a rapid increase to these velocities. The equatorial excretion disk however, is characterized by a slowly increasing outflow, which reaches velocities of the order of only a $\sim$ 100 km s^{-1}. A latitude-dependent wind model for Be and B[e] envelopes was developed by Araújo, Freitas Pacheco, & Petrini (1994). They have allowed the relative contributions from optically thin and thick lines to vary as a function of the star's latitude. Although they have obtained some encouraging results, numerical problems have prevented them from obtaining solutions for the most interesting cases. Chen & Marlborough (1994) have encountered analogous difficulties. More recently Araújo (1995) has obtained accurate solutions for an expansion driven mainly by thin lines.

The goal of the present work is to explore the possibility of an outflow maintained by optically thin lines as a tentative scenario for the equatorial disk of B[e] supergiants. This assumption is discussed in detail again in the paper. We have also included a radiative force term due to electron scattering and a centrifugal force term. Solutions of some cases reveal an outflow with the desired properties, as it will be discussed later. In § 2 the assumptions and equations of our radiation model are described. A particular case, which closely resembles the Parker model for the solar wind, is analyzed in § 3. Application to B[e] supergiant excretion disks is performed in § 4, together with a first discussion of the results. Finally, in § 5, we summarize some conclusions and an outlook on future developments is given.

2. THE MODEL: BASIC ASSUMPTIONS AND EQUATIONS

We shall now revise the model definitions for the sake of completeness (these points have already been detailed in previous works, e.g., Araújo 1995). A complete hydrodynamical approach would require a simultaneous solution of the equations of mass, momentum and energy conservation, together with an equation of state. Mass and momentum conservation are expressed in a vector formalism by

$$\frac{\partial \rho}{\partial t} + \nabla.(\rho \bar{v}) = 0\,, \tag{1}$$

$$\rho\Big(\frac{\partial \bar{v}}{\partial t} + \bar{v}.\nabla\bar{v}\Big) + gradP + \bar{F} + \bar{f} = 0\,. \tag{2}$$

In the above equation ρ is the mean density, $\bar{v}$ is the velocity field, P is the pressure, $\bar{F}$ is the total body force per unit volume and $\bar{f}$ is the boundary force per unit volume acting on the fluid. In view of the uncertainties in the heating and cooling processes, we bypass the energy equation adopting a variation of temperature throughout the envelope of the form

$$T(r) = T_0 \left(\frac{R}{r}\right)^{\beta}\,, \tag{3}$$

where β is an ad-hoc adjustable parameter. We assume also an ideal gas equation of state

$$P = a^2 \rho\,, \tag{4}$$

where a is the isothermal sound speed.

Let us consider a spherical polar coordinate system (r, θ, ϕ) with the center of the star at $r = 0$ and with the equatorial plane at $\theta = \frac{\pi}{2}$. The azimuthal angle is measured in the same sense as star's rotation. By hypothesis, the envelope is in a steady state situation and axial symmetry is imposed. Concerning the velocity field, Bjorkman & Cassinelli (1993) and Owocki, Cranmer, & Blondin (1994) and Owocki, Cranmer, & Gayley (1996) have shown that meridional flows may be relevant in the dynamics of the envelopes of rotating B-type stars. As we are interested in the physical conditions prevailing in the excretion disk of B[e] supergiants we concentrate our analysis to the equatorial region. In such a case we may consider $v_\theta \approx 0$, since $\theta = \frac{\pi}{2}$ is a plane of symmetry.

The above assumptions yield to a direct integration of the mass conservation equation

$$\Phi = r^2 \rho\, v_r\,; \tag{5}$$

where Φ is the mass flux per unit of solid angle. The radial component of the equation of motion will be

$$v_r \frac{\partial v_r}{\partial r} - \frac{{v_\phi}^2}{r} + \frac{1}{\rho}\frac{\partial P}{\partial r} + \frac{GM(1-\Gamma)}{r^2} - \frac{1}{\rho}F^l = 0\,. \tag{6}$$

The second term represents the centrifugal force and the fourth one is the effective gravitational acceleration (including the radiative force due to electronic scattering). The last term is the radiative force due to line opacity. The parameter Γ is given by

$$\Gamma = \frac{\sigma_e L}{4\pi G M c}\,. \tag{7}$$

In this expression σ_e is the electron opacity per unit mass, L is the stellar luminosity and M is the mass of the star. Other symbols have their usual meaning.

The equation for the azimuthal component reduces to

$$v_r \frac{\partial v_\phi}{\partial r} + \frac{v_\phi v_r}{r} = \mathbf{f}\,, \tag{8}$$

where $\mathbf{f}$ is an unknown viscous force per unit mass. Since we still do not have a definite theory for turbulent viscous forces on stellar atmospheres, we adopt as a solution of above equation

$$v_\phi(r) = V\left(\frac{R}{r}\right)^{\delta}, \quad -1 \leq \delta \leq 1\,; \tag{9}$$

where V is the photospheric equatorial velocity (R is the stellar radius) and δ is an empirical viscosity parameter. $\delta = -1$ corresponds to solid body rotation while $\delta = 1$ indicates conservation of specific angular momentum per unit mass. Equation (9) may be rewritten as follows

$$v_\phi(r) = \chi\left(\frac{GM(1-\Gamma)}{R}\right)^{\frac{1}{2}}\left(\frac{R}{r}\right)^{\delta}; \tag{10}$$

χ is the ratio between the centrifugal acceleration and the effective gravity.

Let us examine now the radiative force on lines F^l, which appears in equation (6). Following Friend & Abbott (1986) it may be expressed as

$$\frac{F^l}{\rho} = \frac{\sigma_e L}{4\pi c r^2}\, k t^{-\alpha}\, g(r, v_r, \frac{dv_r}{dr})\,. \tag{11}$$

Here t is an optical depth variable defined by $t = \sigma_e \rho v_{th}\left(dv_r/dr\right)^{-1}$, k and α are named "radiative parameters" and $g(r, v_r, dv_r/dr)$ is a correction which takes into account the size of the star (v_{th} is obviously the thermal velocity). The parameter k is related to the total number of lines driving the wind, while α gives the relative contribution of optically thick and thin lines ($\alpha = 0$ corresponds to no thick lines at all whereas $\alpha = 1$ represents no thin lines).
The correction factor g is

$$g(r, v_r, \frac{dv_r}{dr}) = \frac{1 - \left\{1 - \left(R/r\right)^2\left[1 - \frac{v_r/r}{dv_r/dr}\right]\right\}^{1+\alpha}}{(1+\alpha)\left(R/r\right)^2\left[1 - \frac{v_r/r}{dv_r/dr}\right]} \tag{12}$$

The equation that results for wind expansion (combining (3); (4); (5); (6); (10) and (11)) is

$$\left[v_r - \frac{a_0^2}{v_r}\left(\frac{R}{r}\right)^{2\beta}\right] dv_r/dr + \frac{GM(1-\Gamma)}{r^2}\left[1 - \chi^2\left(\frac{R}{r}\right)^{2\delta-1}\right] =$$

$$= \frac{2a_0^2}{R}(1+\beta)\left(\frac{R}{r}\right)^{2\beta+1} + \frac{C(r/R)^{\beta\alpha}}{r^2}\left(r^2 v_r \frac{dv_r}{dr}\right)^{\alpha} g(r, v, \frac{dv_r}{dr})\,, \tag{13}$$

in which a_0 is the photospheric sound speed. C is an eingenvalue of the solution. It is related to the mass flux by

$$C = \frac{\Gamma GMk}{(\sigma_e v_{th}\Phi)^{\alpha}}\,. \tag{14}$$

This equation is solved numerically by standard techniques. The first step consists in computing the velocity and its derivative at a special point called the critical radius, which is defined by regularity and singularity conditions. Subsequently, we perform a numerical integration from this critical point, obtaining a whole solution $v_r(r)$. For further details in the method of solution the reader is referred to Pauldrach et al. (1986) and Araújo (1995).

3. THE "SOLAR-TYPE" WIND CASE

In this paper, we restrict ourselves to the situation in which the line force is uniquely given by weak (optically thin) lines. In such a case, the value of the radiative parameter α is $\alpha = 0$. For us this is a working hypothesis but it is rather drastic and we will try to justify it a bit more now. Radiation-driven theory for hot/luminous star winds is based on CAK classical work. In their formalism the most significant contribution for the radiative force is given by optically thick lines. This theory has been (more or less) sucessfully addressed to O-type star winds, in which terminal velocities are of the order of 1000–3000 km s^{-1} and there is a rapid increase to such speeds. However, some objects may present qualitatively distinct expansion characteristics, with velocities of only $\approx$ 100–300 km s^{-1}. Among them, the luminous blue variable P-Cygni (and perhaps some other analogous objects) and specially classical Be and B[e] stars.

A CAK-type rotationally-distorted wind model for B[e] supergiant envelopes was developed some years ago by Boyd & Marlborough (1991). They concluded that a denser equatorial plane must be present in order to reproduce continuum linear polarization with reasonable rotational rates. Moreover, they suggested a great number of optically thin lines as an adequate driving mechanism. In fact this possibility had been raised some years before by Lamers (1986) in his study of P-Cygni. Afterwards, Pauldrach & Puls (1990) have shown that a wind may be bi-stable if the optical thickness in the Lyman continuum is close to unity. For optically thin media the degree of ionization will be high, so the radiative force would be mainly produced by lines in the Lyman continuum (for instance O VI, N V and C IV resonant transitions) and the radiative parameter α would be high. The opposite situation is achieved in media which are optically thick in the Ly continuum, with a major contribution of the Fe-group lines. We recall that this behaviour is in qualita-

tive agreement with Abbott's (1982) computations of the radiative force. Most importantly, the transition from one stage of ionization to another may occur with a relatively small change in temperature. Subsequently Lamers & Pauldrach (1991) suggested that a latitude contribution of lines may be generated in rotating B-type stars (and most likely in B[e] supergiants) as a consequence of such a mechanism. More recently, Stee et al. (1995) performed a detailed analysis of the circumstellar matter of the Be star γ Cas on the basis of spectroscopic and interferometric measurements. They have obtained that the terminal velocity should vary with star co-latitude θ, decreasing from ≈ 2000 km s^{-1} in the poles to $\approx$ 200 km s^{-1} at the equatorial plane. In order to reproduce such velocities, the α parameter should vary from ≈ 0.5 (poles) to ≈ 0.1–0.05 (equator), which indicates almost no contribution of thick lines in this last region.

The dynamical problem of equatorial disk formation around rotating B-type stars is a long-standing one. A new paradigm in this context has seemed to appear with the contribution by Bjorkman & Cassinelli (1993), the so-called wind-compressed disk model. Their semianalytic model states that meridional streams would generate, within some conditions, the equatorial disk. At first these results were roughly confirmed by more accurate 2D hydrodynamical simulations (Owocki et al. 1994). However, Owocki et al. (1996) presented opposite results in a very recent work. They have obtained that the inclusion of non-radial components in the line forces (previously not taken into account) can lead to an effective supression of the equatorward flow needed to form the compressed disk. One suggestion cited in this work is that "driving of B-star winds could be limited to optically thin lines". (Another consequence of the wind-compressed disk model would be the formation of a shock cone around the equatorial region. This conclusion is not supported by Owocki et al. (1996) results. Since this point is open at the moment, it will not be commented here.)

In view of the above discussion, we present here a simple model for the equatorial plane in which only thin lines contribute for the radiative force. In such a case the value of the radiative parameter α is $\alpha = 0$. (We are aware that this is a simplifying assumption, since some optically thick lines shall be present in real situations). Therefore, the radiative force will be

$$\frac{F^l}{\rho} = \frac{k\sigma_e L}{4\pi c r^2}\,, \tag{15}$$

(note that $g(r, v_r, dv_r/dr) = 1$) and the eigenvalue C simplifies to $C = \Gamma GMk$.

Then, the expansion equation in the equatorial plane is reduced to

$$\left[v^2 - a_0^2\left(\frac{R}{r}\right)^{2\beta}\right](1/v)\,(dv/dr) \;=$$

$$= \frac{2a_0^2}{R}(1+\beta)\left(\frac{R}{r}\right)^{2\beta+1} - \frac{GM}{r^2}$$

$$\left\{(1-\Gamma)\left[1-\chi^2\left(\frac{R}{r}\right)^{2\delta-1}\right] - k\Gamma\right\}. \tag{16}$$

The above equation is a generalization of the solar wind equation (e.g., Parker 1960), modified by the inclusion of rotation (χ), a continuum radiative force (Γ) and a thin line force ($k\Gamma$). Moreover, its solution depends on the adopted temperature profile (β). Therefore, we have varied 4 parameters (β, χ, δ and k) and analyzed the corresponding results. Some cases are quite simple but others may be rather complex. Neverthless, in all cases there is (at least) one critical point at which the righthand side of the equation vanishes. Therefore, the lefthand side must also vanish and one of the following conditions must be obeyed

$$(i)\;\; \frac{dv}{dr}\Big|_{r=r_c} = 0\,, \tag{17}$$

or

$$(ii)\;\; v(r=r_c) = a_0\left(\frac{R}{r_c}\right)^{\beta} \tag{18}$$

A transsonic expansion requires condition (ii) to be fullfilled. However, it is not always straightforward to obtain the critical radius, its velocity and derivative. In some cases, more than one critical point appears, which greatly complicates the topology of the equations. In the next section we investigate some particular cases and we present the results obtained in the application for B[e] supergiants.

4. APPLICATION TO B[e] SUPERGIANTS: RESULTS AND DISCUSSION

4.1. Stellar and Wind Parameters

We will present and discuss our results in this section. In order to compute solutions of equation (16) one has to introduce values for stellar and wind parameters. We adopted $M = 30\,M_\odot$, $L = 8.0\times10^5\,L_\odot$ and $T_{eff} = 20\,000$ K which lead to a stellar radius R of the order of 75 solar radii and to $\Gamma \approx 0.6$ [see eq. (7)]. These parameters are typical of superluminous B-type stars (Boyd & Marlborough 1991; Araújo et al. 1994) but they are not adequate to the recently defined class of low luminosity B[e] stars. Therefore, our results should be considered only for the massive and luminous B[e] supergiants. Five rates were adopted for the rotational speed: $\chi = 0.0;\ 0.2;\ 0.5;\ 0.7$ and 0.8. Any specific value

would be rather speculative since photospheric lines are not usually seen in the spectra of these objects.

As wind parameters are concerned we have studied the following cases: $\beta = -0.4; 0.0; 0.4$ and $\delta = 0.0; 0.5; 1.0$. As said previously β gives the behaviour of the temperature profile in the envelope. $\beta = 0.0$ simulates an isothermal flow, a positive value for β represents a decreasing temperature with distance to the central star, whereas a negative one is the opposite situation. The δ parameter governs the rotational velocity law. $\delta = 0.5$ corresponds to Keplerian rotation; $\delta = 1.0$ is the angular momentum conservation case while $\delta = 0$ is a more viscous case. Finally, there is k, the radiative parameter related to the number of driving lines. It seems reasonable to expect this number to be correlated with the wind density, which in turn is believed to be enhanced by rotation. Thus k and χ may be somehow linked and some combination of their values could not be realistic. Nevertheless, for the sake of completeness, we have treated k as a free parameter and it was varied from $k = 0.0$ (no lines at all) to a maximum value k_{max} which is given by the physical requirement that the critical point lies outside the stellar surface, i.e., $r_c > R$. The reader is warned that some cases (those with great χ_s and small k_s or vice-versa), must be taken with caution.

4.2. Results

4.2.1. Case 1: $\beta = 0.0; \delta = 0.5$

This situation corresponds to an isothermal expansion with a Keplerian rotational law. The equation is simply

$$(v^2 - a^2)\frac{1}{v}\frac{dv}{dr} = \frac{2a^2}{r} - \frac{GM}{r^2}\left[(1-\Gamma)(1-\chi^2) - k\Gamma\right], \qquad (19)$$

which is strictly analogous to Parker's isothermal solar equation. A transsonic outflow must obey $v = a$ at the sonic point given by

$$r_c = \frac{GM}{2a^2}\left[(1-\Gamma)(1-\chi^2) - k\Gamma\right]. \qquad (20)$$

Table 1 gives the results for several values of χ and k. It may be seen that for a given k, expansion velocities increase with the rotational rate χ. V_{100} is the velocity at 100 stellar radii. The same behaviour is found when χ is fixed and k is increased. This is clearly shown by Figures 1 ($\chi = 0.2$) and 2 ($\chi = 0.7$). In addition, we note that the highest velocities are obtained with $k = k_{max}$. They are about 75 km s^{-1} in all cases, regardless the adopted χ.

4.2.2. Case 2: $\beta = 0.0; \delta = 0.0$

In this case we still have an isothermal flow but we have decreased the parameter δ in order to simulate

TABLE 1

CASE 1: $\beta = 0, \delta = 1/2$

χ	k	r_c (Stellar Radii)	V_{100} (km s^{-1})
0.0	0.0	47.79	31.7
	0.1	37.73	34.4
	0.2	30.66	37.5
	0.3	23.60	41.3
	0.4	16.53	46.1
	0.5	9.46	53.1
	0.6	2.40	67.6
	0.6198	1.00	75.4
0.2	0.0	43.00	32.3
	0.1	35.94	35.1
	0.2	28.87	38.4
	0.3	21.80	42.4
	0.4	14.74	47.6
	0.5	7.67	55.5
	0.5944	1.00	75.4
0.5	0.0	33.59	36.2
	0.1	26.53	39.6
	0.2	19.46	43.9
	0.3	12.40	49.8
	0.4	5.33	59.5
	0.4613	1.00	75.4
0.7	0.0	22.84	41.7
	0.1	15.78	46.7
	0.2	8.71	54.0
	0.3	1.64	71.0
	0.3091	1.00	75.4
0.8	0.0	16.12	46.4
	0.1	9.06	53.6
	0.2	1.99	69.3
	0.2140	1.00	75.4

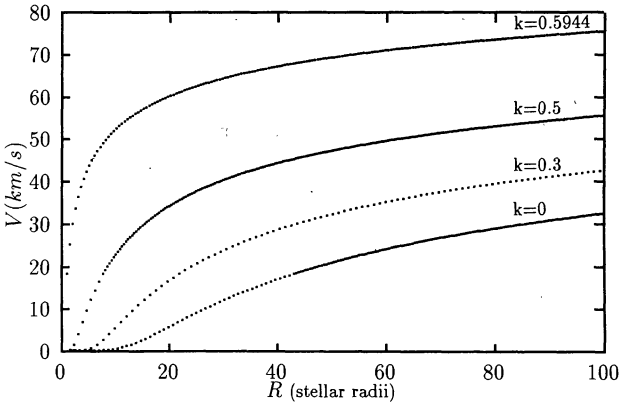

Fig. 1. An example of case 1: for $\chi = 0.2$, expansion velocities increase with k.

a more viscous medium. The expansion equation will be

$$(v^2-a^2)\frac{1}{v}\frac{dv}{dr}=\frac{2a^2}{r}-\frac{GM}{r^2}$$

$$\left\{(1-\Gamma)\left[1-\chi^2\left(\frac{R}{r}\right)^{-1}\right]-k\Gamma\right\}, \quad (21)$$

and the expression for the critical radius

$$r_c=\frac{R[1-\Gamma(1+k)]}{\frac{2a^2R}{GM}+\chi^2(1-\Gamma)}. \quad (22)$$

Inspection of Table 2 shows once again, a positive correlation between outflow velocity and k and/or χ. Furthermore, it seems clear that for $k=k_{max}$ the velocities are almost the same as the previous case ($\delta=0.5$). On the other hand, for $k_s<k_{max}$, the expansion now is higher (see also Figures 3 and 4). Comparing these two cases we may note the relation between the critical point and the resulting velocity. This is not surprising since, in fact, the normalized solution (v in units of a; r in units of r_c) is the same in both cases.

4.2.3. Case 3: $\beta=0.0;\delta=1.0$

The equations for this case are given by

$$(v^2-a^2)\frac{1}{v}\frac{dv}{dr}=\frac{2a^2}{r}-\frac{GM}{r^2}$$

$$\left\{(1-\Gamma)\left[1-\chi^2\left(\frac{R}{r}\right)\right]-k\Gamma\right\}, \quad (23)$$

and

$$r_c=\frac{\frac{GM}{2a^2}[1-\Gamma(1+k)]}{2}\pm$$

$$\frac{\left\{\left(\frac{GM}{2a^2}\right)^2[1-\Gamma(1+k)]^2-\frac{4GM}{2a_0^2}\chi^2R(1-\Gamma)\right\}^{\frac{1}{2}}}{2} \quad (24)$$

From (24) it may be seen that there are two critical radii. This strongly complicates the analysis of (23), and we have been not able to perform the numerical integration.

4.2.4. Case 4: $\beta=0.4;\delta=0.5$

In this case and in the next one we have allowed a temperature variation according to (3), while maintaining a Keplerian rotational law ($\delta=0.5$). Therefore, the temperature decreases with the distance to the star for $\beta>0$ while $\beta<0$ gives an increasing temperature law. The radial momentum equation for both cases may be written as

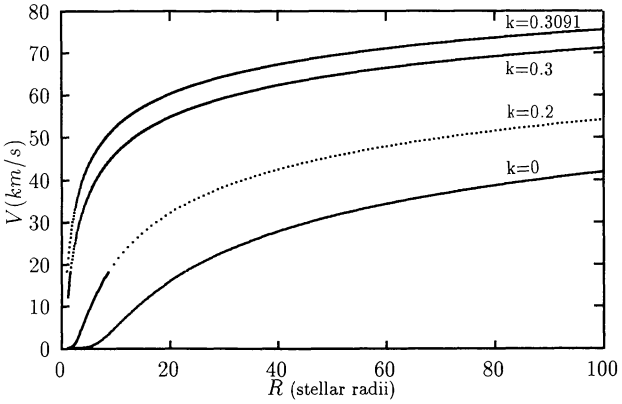

Fig. 2. Here we show the behaviour for $\chi=0.7$. Note that we have the same behaviour of v_{exp} with k but now the expansion velocities for the same k are greater than in Figure 1.

TABLE 2

CASE 2: $\beta=0,\delta=0$

χ	k	r_c (Stellar Radii)	V_{100} (km s^{-1})
0.0	0.0	44.79	31.7
	0.1	37.73	34.4
	0.2	30.66	37.5
	0.3	23.60	41.3
	0.4	16.53	46.1
	0.5	9.46	53.1
	0.6	2.40	67.6
	0.6198	1.00	75.4
0.2	0.0	16.04	46.6
	0.1	13.51	48.7
	0.2	10.98	51.2
	0.3	8.45	54.4
	0.4	5.92	58.4
	0.5	3.39	64.2
	0.5944	1.00	75.4
0.5	0.0	3.67	63.4
	0.1	3.09	65.1
	0.2	2.51	67.2
	0.3	1.93	69.6
	0.4	1.35	72.8
	0.4613	1.00	75.4
0.7	0.0	1.95	69.5
	0.1	1.64	71.1
	0.2	1.33	72.9
	0.3	1.02	75.2
	0.3091	1.00	75.4
0.8	0.0	1.50	71.9
	0.1	1.27	73.4
	0.2	1.03	75.2
	0.2140	1.00	75.4

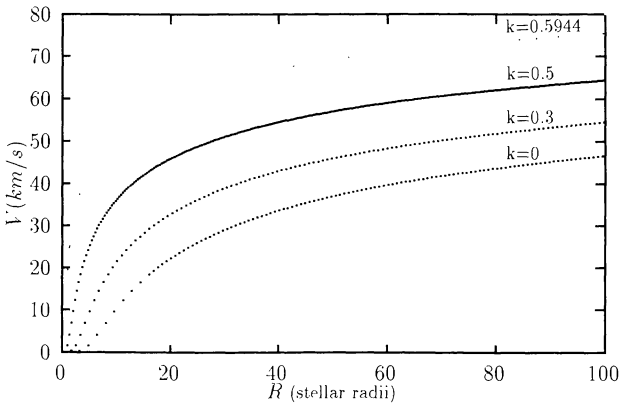

Fig. 3. An example of case 2 with $\chi = 0.2$. Its behaviour is the same to that of case 1 but with a higher expansion.

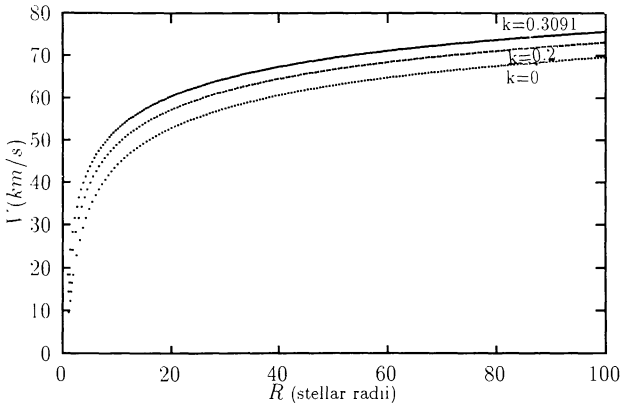

Fig. 4. Another example of case 2 with $\chi = 0.7$.

$$\left[v^2 - a_0^2\left(\frac{R}{r}\right)^{2\beta}\right]\frac{1}{v}\frac{dv}{dr} = \frac{2a_0^2}{R}(1+\beta)\left(\frac{R}{r}\right)^{2\beta+1} - \frac{GM}{r^2}\left[(1-\Gamma)(1-\chi^2) - k\Gamma\right], \quad (25)$$

and the critical point expression is

$$r_c = \left\{\frac{GM[(1-\Gamma)(1-\chi^2) - k\Gamma]}{2a_0^2(1+\beta)R^{2\beta}}\right\}^{\frac{1}{1-2\beta}}. \quad (26)$$

Results for case 4 are in Table 3. Terminal velocities are again of the order of 75 km s^{-1}, when $k \approx k_{max}$. However, for small k_s, critical radii are indeed large. The corresponding velocities are so small that they could not be accurately determined. They appear as asterisk marks in Table 3.

TABLE 3

CASE 4: $\beta = 0.4, \delta = 1/2$

χ	k	r_c (Stellar Radii)	V_{100} (km s^{-1})
0.0	0.0	$3.35\,10^7$	...
	0.1	$1.42\,10^7$	...
	0.2	$5.04\,10^6$	...
	0.3	$1.36\,10^6$	...
	0.4	$2.30\,10^5$	...
	0.5	$1.41\,10^4$	...
	0.6	$1.40\,10^1$	...
	0.6141	$1.00\,10^0$	75.4
0.2	0.0	$2.73\,10^7$	...
	0.1	$1.12\,10^7$	...
	0.2	$3.73\,10^6$	...
	0.3	$9.17\,10^5$	...
	0.4	$1.29\,10^5$	...
	0.5	$4.95\,10^3$	...
	0.5888	$1.00\,10^0$	75.3
0.5	0.0	$7.96\,10^6$	...
	0.1	$2.44\,10^6$	...
	0.2	$5.20\,10^5$	...
	0.3	$5.45\,10^4$	...
	0.4	$8.03\,10^2$	...
	0.4556	$1.00\,10^0$	74.7
0.7	0.0	$1.16\,10^6$	...
	0.1	$1.82\,10^5$	...
	0.2	$9.35\,10^3$	...
	0.3	$2.26\,10^0$	49.1
	0.3021	$1.00\,10^0$	75.2
0.8	0.0	$2.03\,10^5$	...
	0.1	$1.14\,10^4$	...
	0.2	$5.87\,10^0$	28.8
	0.2084	$1.00\,10^0$	75.2

4.2.5. Case 5: $\beta = -0.4; \delta = 0.5$

This last case has presented interesting new results (see Table 4). Significant changes have not occurred for $k = k_{max}$, but the positive correlation between expansion velocity and k (shown in previous cases) is not seen now. In fact we have adopted now a temperature law which increases with distance to the star and decreasing velocities were obtained for increasing χ and k. Furthermore, greater velocities are reached for small k_s: $V_{100} \approx 110 - 130$ km s^{-1}. This behaviour, illustrated in Figures 5 and 6, is a consequence of the decrease of the sound speed at the critical point since higher k moves this point inward in the wind where the temperature is lower.

TABLE 4

CASE 5: $\beta = -0.4, \delta = 1/2$

χ	k	r_c (Stellar Radii)	V_{100} (km s^{-1})
0.0	0.0	11.00	133.6
	0.1	9.98	131.5
	0.2	8.89	128.9
	0.3	7.68	125.4
	0.4	6.30	120.6
	0.5	4.62	112.6
	0.6	2.16	93.3
	0.6254	1.00	75.6
0.2	0.0	10.70	133.1
	0.1	9.71	130.9
	0.2	8.60	128.0
	0.3	7.36	124.3
	0.4	5.92	118.9
	0.5	4.12	109.6
	0.6001	1.00	75.5
0.5	0.0	9.35	130.1
	0.1	8.20	127.0
	0.2	6.91	122.8
	0.3	5.37	116.5
	0.4	3.36	104.5
	0.4669	1.00	75.6
0.7	0.0	7.55	125.1
	0.1	6.15	119.8
	0.2	4.42	111.5
	0.3	1.75	88.2
	0.3148	1.00	75.5
0.8	0.0	6.22	120.2
	0.1	4.51	112.0
	0.2	1.94	90.8
	0.2197	1.00	75.5

5. CONCLUSIONS

In this paper we have presented a rotationally-distorted radiative wind model driven by optically thin lines and electronic scattering. Our aim was to verify if such a model could reproduce the low expansion outflow ($V_{exp} \leq 100$ km s^{-1}) seen in the equatorial disks of B[e] supergiants.

Velocities at a hundred stellar radii (V_{100}) in the range 40 – 130 km s^{-1} were obtained. Thus, our results seem to indicate that these models should not be discarded at this stage of investigation. Figures 7 and 8 show V_{100} as a function of rotational rate χ for $k = 0.1$ and $k = 0.2$, respectively. We can see that only case 5 lead to terminal velocities greater

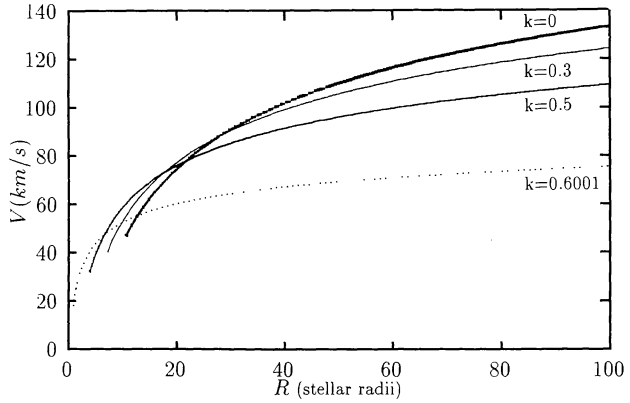

Fig. 5. An example of case 5: with χ for $\chi = 0.2$ higher velocities are obtained for lower values of k. As in other cases we have $v_{100} \approx 75$ km s^{-1} for $k = k_{max}$.

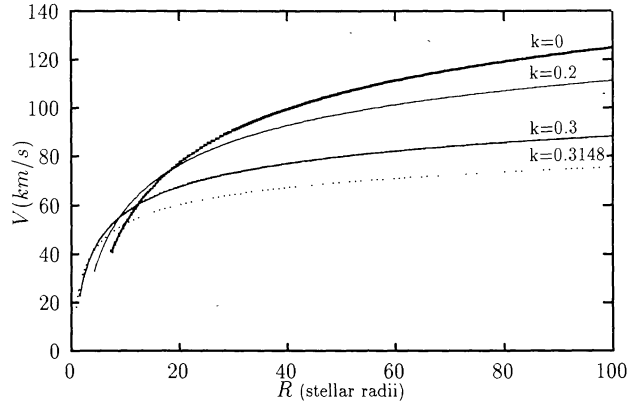

Fig. 6. In the case of a temperature law which increases with distance to the star we have decreasing velocities with χ and k. Here we show this behaviour for $\chi = 0.7$.

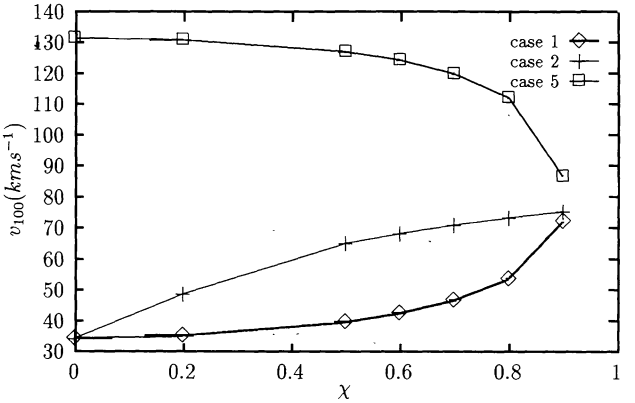

Fig. 7. The behaviour of v_{100} with χ for $k = 0.1$. Cases 1, 2, and 5 are presented.

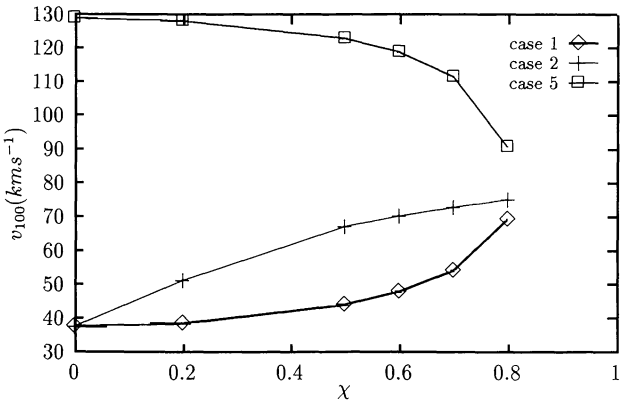

Fig. 8. Here we have fixed $k = 0.2$. The behaviour is very similar to that of Figure 7.

than 100 km s^{-1}. This situation however, would require a better understanding of the cooling and heating mechanisms in the envelope in order to give support to an increasing temperature law. On the other hand, cases 1 and 2 give V_{100} of about 75 km s^{-1} when large values are adopted for k (k_{max}), which implies a great number of thin lines. This velocity is quite acceptable in view of the uncertainties in stellar parameters (mass, radius, luminosity).

Several points should be improved in future studies. We shall deal with more complex numerical cases, like that mentioned in subsection 4.2.3. Another step would be to admit a small contribution from optically thick lines. This situation may be simulated by changing the α parameter from $\alpha = 0.0$ to $\alpha = 0.1-0.2$. However, a non-zero value of α makes the numerical solution of the equation much more difficult and more powerful methods must be employed (see Araújo 1995). A major improvement would consist in introducing explicitly the energy conservation equation, whose solution would give us the temperature law in the excretion disk. Finally, a realistic, self-consistent method, would require a simultaneous computation of the radiative force parameters α and k as a function of star's latitude, in a time-dependent, 2D hydrodynamical model.

REFERENCES

Abbott, D. C. 1982, ApJ, 259, 282
Araújo, F. X. 1995, A&A, 298, 179
Araújo, F. X., Freitas Pacheco, J. A., & Petrini, D. 1994, MNRAS, 267, 501
Bjorkman, J. E., & Cassinelli, J. P. 1993, ApJ, 409, 429
Boyd, C. J., & Marlborough, J. M. 1991, ApJ, 369, 191
Castor, J. I., Abbott, D. C., & Klein, R. I. 1975, ApJ, 195, 157
Chen, H., & Marlborough, J. M. 1994, ApJ, 427, 1005
Friend, D., & Abbott, D. C. 1986, ApJ, 311, 701
Gummersbach, C. A., Zickgraf, F.-J., & Wolf, B. 1995, A&A, 302, 40
Lamers, H.J.G.L.M. 1986, A&A, 159, 90
Lamers, H.J.G.L.M., & Pauldrach, A. 1991, A&A, 244, L5
Owocki, S. P., Cranmer, S. R., & Blondin, J. M. 1994, ApJ, 424, 887
Owocki, S. P., Cranmer, S. R., & Gayley, K. G. 1996, ApJ, 472, L115
Parker, E. N. 1960, ApJ, 132, 175
Pauldrach, A., & Puls, J. 1990, A&A, 237, 424
Pauldrach, A., Puls, J., & Kudritzki, R. P. 1986, A&A, 164, 86
Stee, Ph., Araújo, F. X., Vakili, F., Mourard, D., Arnold, L., Bonneau, D., Morand, M., & Tallon-Bosc, I. 1995, A&A, 300, 219
Waters, L.B.F.M., & Marlborough, J. M. 1994, in Pulsation, Rotation and Mass-Loss in Early-type Stars, ed. L. A. Balona, H. F. Henrichs, & J. M. Le Contel, (Dordrecht: Kluwer), 399
Zickgraf, F.-J. 1989, in Angular Momentum and Mass Loss for Hot Stars, ed. L. A. Willson & R. Stalio, (Dordrecht: Kluwer), 245
_____. 1993, in New aspects of Magellanic Cloud Research, ed. B. Baschek, G. Clare, & J. Lequeux, (Berlin: Springer), 257
Zickgraf, F.-J., Wolf, B., Stahl, O., Leitherer, C., & Appenzeller, I. 1986, A&A, 163, 119

F. X. de Araújo and A. R. R. de Carvalho: CNPq-Observatório Nacional, DAGE, Rua José Cristino 77, 20921-400, Rio de Janeiro, Brazil (araujo@obsn.on.br).